RSC Advances

ROYAL SOCIETY OF CHEMISTRY

www.rsc.org/advances

Enhancement of the advanced Fenton process by weak magnetic field for the degradation of 4-nitrophenol

Xinmei Xiong,[a,b] Yuankui Sun,[a] Bo Sun,[a] Weihua Song,[c] Jingyi Sun,[a] Naiyun Gao,[a] Junlian Qiao,[a] Xiaohong Guan[a,*]

[a]State Key Laboratory of Pollution Control and Resources Reuse, College of Environmental Science and Engineering, Tongji University, Shanghai 200092, P. R. China

[b]Department of Civil Engineering, Jiujiang University, Jiujiang 332005, Jiangxi, China

[c]Department of Environmental Science & Engineering, Fudan University, Shanghai, P. R. China

*Corresponding author contact information:

Xiaohong Guan, Email: guanxh@tongji.edu.cn, Phone: +86-21-65980956

Abstract

Weak magnetic field (WMF) was employed to enhance the degradation of 4-nitrophenol (4-NP) by advanced Fenton process (Fe^0/H_2O_2) in this study. Although the oxidation rates of 4-NP by Fe^0/H_2O_2 and WMF-Fe^0/H_2O_2 dropped sharply with elevating initial pH (pH_{ini}), the introduction of WMF could remarkably improve the 4-NP degradation by Fe^0/H_2O_2 at pH_{ini} ranging from 3.0 to 6.0. The quenching and electron paramagnetic resonance experiments verified that hydroxyl radical was the primary oxidant responsible for the 4-NP degradation at pH_{ini} 4.0 and the cumulative concentration of $HO^{\bullet}$ in WMF-Fe^0/H_2O_2 system was about 3-fold of that in Fe^0/H_2O_2 system. The superimposed WMF increased the generation of $HO^{\bullet}$ in Fe^0/H_2O_2 process by accelerating the Fe^0 corrosion and Fe^{II} generation, which was the limiting step of Fe^0/H_2O_2 process. The application of WMF largely enhanced the mineralization of 4-NP but it did not change the 4-NP degradation pathways, which were proposed based on the degradation products detected with LC-MS/MS. The optimum intensity of the magnetic field for 4-NP oxidation by WMF-Fe^0/H_2O_2 was determined to be 20 mT. Response surface methodology (RSM) was applied to analyze the experimental variables and it was found that lower pH and higher Fe^0 and H_2O_2 dosages were beneficial for 4-NP degradation by WMF-Fe^0/H_2O_2. Among the three factors (pH_{ini}, Fe^0 dosage, and H_2O_2 dosage) investigated, pH_{ini} was the most important factor affecting the performance of WMF-Fe^0/H_2O_2 process. The WMF-Fe^0/H_2O_2 technology provides a new alternative to scientists working in the field of water treatment.

Keywords: Advanced oxidation process, Hydroxyl radical, Degradation pathway, Mineralization, Response surface methodology

1. Introduction

The classic Fenton process involves aqueous ferrous ions (Fe^{II}) and H_2O_2 that react together to form the highly reactive $HO^{\bullet}$ under acidic condition, as shown in Eq. 1 (in acidic solution, Fe^{II} is usually present as Fe^{2+} and Fe^{III} may be present as $FeOH^{2+}$).[1, 2]

$$Fe^{II} + H_2O_2 \rightarrow Fe^{III} + OH^- + HO^{\bullet} \qquad k_1 = 63.0\ M^{-1}\ S^{-1} \qquad (1)$$

The formed Fe^{III} can be transformed to Fe^{II} following Eqs. (2-3).[1, 2]

$$FeOH^{2+} \rightarrow Fe^{II} + HO_2^{\bullet} \qquad k_2 = 2.7 \times 10^{-3}\ S^{-1} \qquad (2)$$

$$FeOH^{2+} + HO_2^{\bullet} \rightarrow Fe^{II} + O_2 + H^+ \qquad k_3 < 2 \times 10^{3}\ M^{-1}\ S^{-1} \qquad (3)$$

Reaction (1) is the fast step of the Fenton process, while the conversion of Fe^{III} to Fe^{II} (Eqs. (2-3)) is considerably slower. Therefore, the Fe^{II} concentration in classic Fenton process decreases sharply and a very fast first step followed by a considerable slowing down of the reaction is often observed.[3] The main shortcomings associated with this technology are related with the narrow effective pH range (2.5−3.0) with the optimum pH for Fenton at 2.8,[4] the requirement of high amount of the homogeneous catalyst (ferrous iron salts), and generation of large amount of iron containing sludge which has to be separated and disposed.[5]

An improvement in the Fenton process is the advanced Fenton process (AFP), which uses zero-valent iron (Fe^0) to replace ferrous iron salts.[2, 6] Initially, Fe^0 is oxidized via a two electron transfer from the particle surface to H_2O_2 following Eq. 4 and Fe^{II} is generated.[7] The Fe^{II} reacts rapidly with H_2O_2 to produce hydroxyl radicals via Eq. 1, and in the meantime generate Fe^{III}, which is then reduced to Fe^{II} by further

interaction with the Fe^0 surface following Eq. 5 at a faster rate compared to the homogeneous process.[8, 9]

$$Fe^0 + 2H^+ \rightarrow Fe^{II} + H_2 \quad (4)$$

$$Fe^0 + 2FeOH^{2+} \rightarrow 3Fe^{II} + 2OH^- \quad (5)$$

Compared to the classic Fenton process, AFP avoids the addition of counteranions (Cl^- or SO_4^{2-}) to the treated system[10] and the amount of iron-containing precipitates generated in AFP is significantly lower than that in the classical Fenton process.[5, 8] However, the performance of AFP is limited by the amount of Fe^{II} available to catalyze H_2O_2 and additional assistants such as UV[8] or visible light irradiation[11] and ultrasound[12] have been proposed to enhance contaminants removal by AFP. Nanoscale Fe^0 has also been proposed to replace the microscale Fe^0 to catalyze H_2O_2 so as to improve the performance of AFP.[7, 13] Despite much effort has been made to enhance the AFP, much room still remains for improving the cost-effectiveness and easy operation of this technology.

It has been generally believed that only magnetic field (MF) with high intensity (>2 T) affects chemical reactions[14] and this viewpoint prevents the application of MF in water and wastewater treatment. Recently, it was found in our lab that the application of an inhomogeneous weak magnetic field (WMF) (B_{max} < 20 mT) could significantly enhance Se(IV) removal by both pristine Fe^0 and aged Fe^0 [15, 16] and greatly improve As(V) and As(III) removal by Fe^0 at pH_{ini} 3.0−9.0.[17] The accelerated Se(IV), As(III) and As(V) removal by Fe^0 was mainly ascribed to the improved Fe^0 corrosion and Fe^{II} generation. Consequently, WMF and Fe^0 were employed to activate

persulfate (PS) synergistically and it was found that the applied WMF induced a significant enhancement in the removal rates of organic contaminants by Fe^0/PS.[10] Therefore, a hazardous and refractory aromatic compound 4-nitrophenol (4-NP) was selected as the model compound to explore the possibility of employing WMF to enhance 4-NP degradation by AFP in this work.

The response surface methodology (RSM), which had been widely employed for the optimization of the Fenton process as well as in other catalytic studies,[18] was employed to evaluate the relative significance of several independent factors and predict the optimum operating conditions for desirable responses in this study. The Box-Behnken experimental design (BBD), a modified central composite experimental design with excellent predictability,[19] was employed to investigate the effect of initial pH (pH_{ini}), H_2O_2 dosage and Fe^0 dosage on the removal efficiency of 4-NP by WMF assisted AFP (WMF-Fe^0/H_2O_2).

Therefore, the objectives of this study were to 1) investigate the feasibility of applying WMF to enhance 4-NP degradation by Fe^0/H_2O_2 process at various pH_{ini} and MF intensities; 2) explore the mechanism of enhanced 4-NP degradation in WMF-Fe^0/H_2O_2 process; 3) determine the key parameters (pH, Fe^0 dosage, H_2O_2 dosage) affecting the WMF-Fe^0/H_2O_2 process by employing the RSM with BBD; 4) analyze the possible degradation pathways and mineralization of 4-NP in both Fe^0/H_2O_2 and WMF-Fe^0/H_2O_2 systems.

2. Experimental

2.1. Chemicals

4-NP, benzoic acid (BA), p-hydroxybenzoic acid (p-HBA), and 5,5-dimethyl-1-pyrroline-1-oxide (DMPO) were reagent grade while methanol, acetonitrile, and formic acid were HPLC grade. These chemicals were purchased from J&K Chemical Co.. Fe^0 powder (⩾98% pure, and BET surface area 0.87 m^2 g^{-1}) were obtained from Shanghai Jinshan smelter (Shanghai, China). The Fe^0 particles were agglomerated with D_{50} of ~24.9 μm, as shown in Fig. S1. H_2O_2 (30%) and other chemicals employed were obtained from the Sinopharm Group Chemical Reagent Co., Ltd. (Shanghai, China). All solutions were prepared with high-purity water obtained from a Millipore Milli-Q system with resistivity＞18 MΩ cm at 25 ^oC.

2.2. Magnetic Fields (MFs)

Two different forms of MFs, one was uniform and the other was nonuniform, were adopted in this study. The nonuniform MF was generated by positioning two thin cylindrical neodymium-iron-boron permanent magnets under the water bath, as illustrated in Fig. S2. The intensity of the MF was determined with a Teslameter (HT201, Shanghai Hengtong Magnetic & Electric Technology Co., Ltd) to be 10-40 mT at the bottom of the reactor. The uniform MF was offered by an electromagnetic field generator (EM5-C, East Changing Technology Co., Ltd., China) with MF intensity range < 1 T. To investigate the influence of MF intensity on 4-NP degradation in WMF-Fe^0/H_2O_2 process, the uniform MF was employed. Otherwise, the nonuniform MF was applied.

2.3. Experimental Procedures

All experiments were performed open to the air in a series of borosilicate glass

jars under constant stirring rate (400 rpm) with a mechanical stirrer (D2004W, Shanghai Sile Instrument Co., Ltd). With this stirring intensity, Fe^0 could be evenly distributed in the solution and no aggregation of Fe^0 was observed at the bottom of the reactor in the MF. The influence of MF intensity on 4-NP degradation by Fe^0/H_2O_2 process was determined at room temperature. All the other experiments were carried out at 25 ± 1 °C, which was controlled with a water bath.

Each 500 mL unbuffered reaction solution with desired concentrations of 4-NP (0.02 mM) and H_2O_2 (0.1-1.0 mM) was prepared and adjusted to the pre-determined pH_{ini} with sulfuric acid and sodium hydroxide. Experiments were initiated immediately once Fe^0 (0.1-1.0 mM) powder was dosed into the reactor. Samples were withdrawn at predetermined time intervals and quenched by methanol (for 4-NP analysis) or sodium sulfite (for TOC analysis). The samples were filtered through a 0.22 μm membrane filter (PES) before analysis. Electron paramagnetic resonance (EPR) experiments were carried out at room temperature on an EPR spectrometer (Bruker A200 ESP 300E instrument at 300K) and the details are presented in Text S1. All experiments were run in duplicate, batch mode and the data were reported as the mean of the two replicates with error bars.

2.4. Chemical Analysis

The concentrations of 4-NP and p-HBA were analyzed by UPLC (Waters) with a Symmetry C18 column (2.1*100 mm, 1.7 μm) and UV-visible detector. 4-NP was detected at a wavelength of 318 nm with an isocratic method (H_2O:MeOH = 60:40) at t_R = 3.09 min, while p-HBA was detected at a wavelength of 255 nm with an isocratic

method (H_2O:Acetonitrile = 10:90) at t_R = 1.57 min. The concentration of H_2O_2 was determined by the potassium titaniumoxalate method (detection limit: 0.1 mg L^{-1}) using a UV-Vis spectrophotometer at 400 nm (TU1902, Universal Analysis, Beijing, China).[20] The concentrations of ferrous and ferric ion (after reduction to Fe^{II} with hydroxylamine hydrochloride) were determined on UV-Vis spectrophotometer at 510 nm after complexing with 1,10-phenanthroline (detection limit: 0.03 mg L^{-1}).

TOC was monitored using a TOC analyzer (L-CPH CN200, Shimadzu). In order to ensure the accurate measurement of TOC, the initial concentration of 4-NP was increased to 100 μM and the dosages of both Fe^0 and H_2O_2 were correspondingly elevated to 2.5 mM. UPLC together with electrospray-ionization Quadruple Time-of-Flight tandem mass spectrometry (UPLC-ESI-QTOF MS), Waters Acquity UPLC-Xevo G2 QTOF, was used to detect the intermediates of 4-NP degradation. In this study, the mass spectrometer was operated in the *m/z* range of 50-300. The eluent was delivered at 0.4 mL min^{-1} by a gradient system (Table S1) with a C18 column 2.1 mm*100 mm, 1.7 μm, 45 ^oC.

The strength and gradient of MF induced by Fe^0 particles were characterized using an Finite element calculation software, assuming that a pure Fe^0 sphere with diameter of 10 μm was exposed to an external uniform MF with flux density of 5, 10, or 20 mT and the relative magnetic permeability of the Fe^0 sphere is 1700.

2.5. Experimental design

RSM based on BBD was applied to investigate the effects of the three independent variables on the response function. The independent variables were pH

(A), Fe^0 dosage (B) and H_2O_2 dosage (C). The low, center and high levels of each variable were designated as -1, 0 and +1, respectively, as illustrated in Table S2, which were selected based on available resources and preliminary experiments. The square-root of k_{obs} (the pseudo first-order rate constants of 4-NP degradation) was chosen for the response factor (Y) in order to ensure that the predicted k_{obs} values are greater than zero.

$$\ln {}^{C}/_{C_0} = -k_{obs}t \quad (6)$$

The mathematical relationship between the response function (Y) and the independent variables (A, B, C) can be approximated by a quadratic polynomial equation as follows:

$$Y = b_0 + b_1A + b_2B + b_3C + b_{12}AB + b_{13}AC + b_{23}BC + b_{11}A^2 + b_{22}B^2 + b_{33}C^2 \quad (7)$$

where Y is the response and A, B, C, AB, AC, BC, A^2, B^2, and C^2 are the independent variables' effects, square effects and interaction effects; b_i, b_{ij} and b_{ii} are the linear coefficients, interaction coefficients and squared coefficients; b_0 is the intercept parameter.[21] The software design expert 8.0.6 was used for experimental design, determination of the coefficients and data analysis.

3. Results and discussion

3.1. Effect of WMF on 4-NP removal by Fe^0/H_2O_2 at different pH_{ini} levels

Only ~3.0% of 4-NP could be removed by H_2O_2 alone or Fe^0 alone at pH_{ini} 4.0 in 2 h without WMF, as shown in Fig. S3(a). The application of WMF had no influence on 4-NP degradation by H_2O_2 but slightly enhanced 4-NP sequestration by Fe^0 from ~3.0% to ~8.0% at pH_{ini} 4.0 in 2 h, as illustrated in Fig. S3. The slight improvement in

4-NP removal by Fe^0 due to the introduction of WMF should be mainly ascribed to the enhanced Fe^0 corrosion with WMF.[15, 16] The simultaneous application of 0.5 mM Fe^0 and 0.5 mM H_2O_2 could remove ~60.0% 4-NP at pH_{ini} 4.0 within 60 min even without WMF, indicating the high catalytic ability of Fe^0 to H_2O_2 activation, as demonstrated in Fig. S4(b). Surprisingly, 4-NP was completely removed within 60 min in WMF-Fe^0/H_2O_2 process at pH_{ini} 4.0, implying the feasibility of employing WMF to improve the performance of Fe^0/H_2O_2 process.

It is well known that pH plays a key role in the performance of the Fenton process because it affects the solubility of Fe^{II}/Fe^{III}, and ultimately controls the production of hydroxyl radicals. Thus, the kinetics of 4-NP degradation at pH_{ini} ranging from 3.0 to 6.0 in both Fe^0/H_2O_2 and WMF-Fe^0/H_2O_2 systems were determined and demonstrated in Fig. S4. During the reaction process, the change of solution pH value was less than ± 0.3 (data were not shown). The rates of 4-NP degradation drastically decreased with the increase of pH_{ini} in both systems, agree with the phenomena reported in literatures.[5, 22] However, the drop in 4-NP degradation rates in Fe^0/H_2O_2 process with elevating pH was more considerable than those in WMF-Fe^0/H_2O_2 process. Negligible 4-NP was removed by Fe^0/H_2O_2 at pH_{ini} 6.0 in 3 h while 36.8% of 4-NP could be decomposed by its counterpart with WMF in 3 h. Moreover, more 4-NP was removed by WMF-Fe^0/H_2O_2 at pH_{ini} 6.0 than by Fe^0/H_2O_2 at pH_{ini} 5.0 in 3 h, indicating that the WMF-Fe^0/H_2O_2 process had a stronger oxidation activity and a wider effective pH range compared to the Fe^0/H_2O_2 process. This was of great significance in real practice since less pH adjustment was necessary to

achieve a similar removal efficiency of organic contaminant by WMF-Fe^0/H_2O_2 process than by Fe^0/H_2O_2 process.

The loss of 4-NP in both Fe^0/H_2O_2 and WMF-Fe^0/H_2O_2 systems could be simulated with the pseudo-first order kinetics (Eq. 6). The influence of WMF on k_{obs} of 4-NP oxidation by Fe^0/H_2O_2 over the pH_{ini} range of 3.0−6.0 is shown in Fig. 1(a). The rate constants of 4-NP oxidation by WMF-Fe^0/H_2O_2 at pH_{ini} 3.0−5.0 were 1.6−7.9 folds of those by Fe^0/H_2O_2. Furthermore, the rate constant of 4-NP degradation by WMF-Fe^0/H_2O_2 at pH_{ini} 6.0 was 2.2 fold of that by Fe^0/H_2O_2 at pH_{ini} 5.0, further confirming the application of WMF could widen the working pH range of Fe^0/H_2O_2. The influence of WMF on the mineralization of 4-NP by Fe^0/H_2O_2 was assessed by measuring the drop in TOC with an initial 4-NP concentration of 0.10 mM or 7.2 mg L^{-1} TOC at pH_{ini} 4.0. At the end of 3 h, 41% of 4-NP was mineralized by Fe^0/H_2O_2, as shown in Fig. 1(b). However, it took only 1 h to achieve a mineralization rate of 41% in the WMF-Fe^0/H_2O_2 process. Therefore, the application of WMF accelerated not only the 4-NP degradation but also its mineralization. Even in the presence of WMF, about 50% of TOC could not be removed by Fe^0/H_2O_2 process at the end of reaction, indicating that some degradation products of 4-NP were very refractory.

Figure 1.

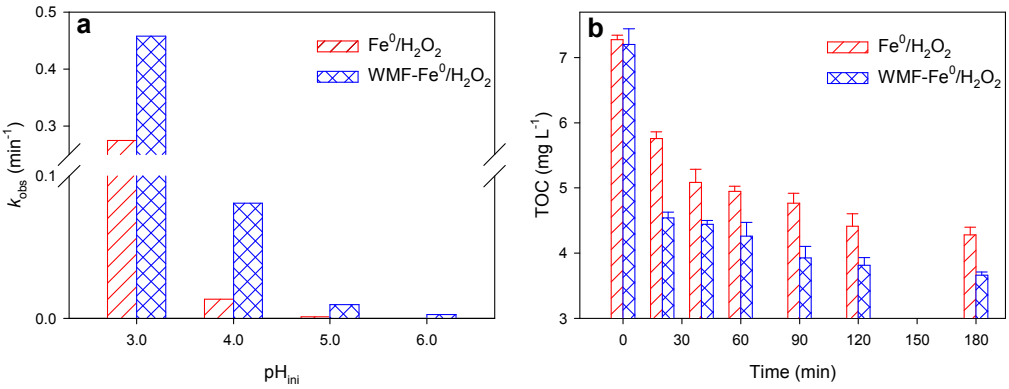

3.2. Role of WMF in the WMF-Fe^0/H_2O_2 process

Tert-Butyl alcohol (TBA) is an efficient scavenger of $HO^{\bullet}$ (k = 6.0×10^8 M^{-1} s^{-1}) but is believed to be less reactive toward high-valent oxoiron complexes like Fe(IV).[23] Figure 2(a) shows that only ~4.5% 4-NP was degraded at pH_{ini} 4.0 in both Fe^0/H_2O_2 and WMF-Fe^0/H_2O_2 systems after dosing excessive TBA, implying that $HO^{\bullet}$ was the dominant active species responsible for the oxidation of 4-NP in the Fe^0/H_2O_2 system, regardless of the presence or absence of WMF. The minor removal of 4-NP in the presence of excessive TBA at pH_{ini} 4.0 indicated that 4-NP may be removed in another way besides $HO^{\bullet}$ oxidation, which was verified by analyzing the reaction intermediates. However, the degradation of 4-NP at pH_{ini} 6.0 was only partially inhibited by TBA, as illustrated in Fig. S5, which indicated that both $HO^{\bullet}$ and Fe(IV) were active oxidative species at near neutral pH.[24]

Figure 2.

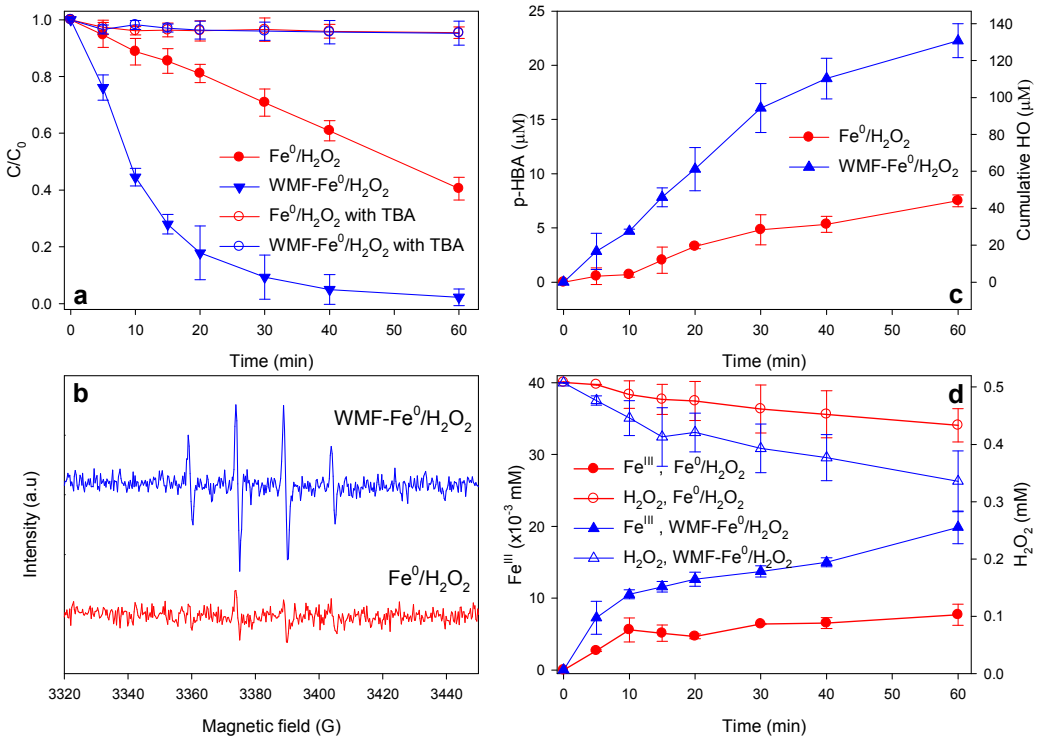

To verify the formation of $HO^{\bullet}$ at pH_{ini} 4.0 in both Fe^0/H_2O_2 and WMF-Fe^0/H_2O_2 systems, EPR tests with DMPO were performed to detect $HO^{\bullet}$ by measuring the intensity of the DMPO-OH adducts signal.[25] As shown in Fig. 2(b), the specific spectra characteristic of DMPO-OH adduct (quartet lines with peak height ratio of 1:2:2:1) were detected in both Fe^0/H_2O_2 and WMF-Fe^0/H_2O_2 systems. However, the intensity of DMPO-OH adduct signal in WMF-Fe^0/H_2O_2 process was much stronger than that in Fe^0/H_2O_2 process, indicating that applying a WMF could greatly enhance the generation of $HO^{\bullet}$. This result was further verified by estimating the cumulative $HO^{\bullet}$ production in both systems. BA could be transformed into three isomers of hydroxybenzoic acid by $HO^{\bullet}$ reaction. The three isomers of hydroxybenzoic acid account for 90 ± 5% of the products with the ratio of o-HBA, m-HBA, and p-HBA products reported to be 1.7:2.3:1.2.[26] For the oxidation of BA by solution-phase $HO^{\bullet}$, the concentration of p-HBA can be used to estimate cumulative $HO^{\bullet}$ production using

Eq. (8):[27]

cumulative $HO^{\bullet}$ produced = [p-HBA] × 5.87 (8)

As shown in Fig. 2(c), the cumulative concentration of $HO^{\bullet}$ in WMF-Fe^0/H_2O_2 system was about 3-fold of that in the Fe^0/H_2O_2 system in 60 min. The enhanced $HO^{\bullet}$ generation was accompanied with the accelerated decomposition of H_2O_2 and generation of Fe^{III}, as illustrated in Fig. 2(d). A close inspection of the data revealed that the concentration of Fe^{III} detected in the WMF-Fe^0/H_2O_2 system was always ~2 times of that in Fe^0/H_2O_2 system. In addition, the amount of decomposed H_2O_2 in the presence of WMF was ~2 fold of that in the absence of WMF. No Fe^{II} was detected through the whole experiments in both Fe^0/H_2O_2 and WMF-Fe^0/H_2O_2 systems, implying that Fe^{II} was immediately oxidized by H_2O_2 after it was released from Fe^0. However, the consumption rate of H_2O_2 does not equal to the generation rate of $HO^{\bullet}$ because H_2O_2 can be decomposed to water and oxygen via the non-radical-producing pathway. The utilization efficiency of H_2O_2 (the molar ratio of generated $HO^{\bullet}$ to consumed H_2O_2) was calculated to be 79.5% in WMF-Fe^0/H_2O_2 process, whereas it was only 65.9% in Fe^0/H_2O_2 process. Therefore, the superimposed WMF also improved the utilization efficiency of H_2O_2 in Fe^0/H_2O_2 process.

The above results confirmed that Fe^0 was the source of Fe^{II}, which catalyzed H_2O_2 in the Fe^0/H_2O_2 system to produce $HO^{\bullet}$ following Eq. 1, and releasing of Fe^{II} from Fe^0 was the limiting step in the Fe^0/H_2O_2 system. An external WMF could enhance the corrosion of Fe^0, accelerating the generation of Fe^{II} and thus leading to an increase in $HO^{\bullet}$ concentration, consistent with the observations reported in our

previous studies.[15-17] Due to its ferromagnetic property, Fe^0 is magnetized in a superimposed WMF and generates an induced inhomogeneous MF, which is stronger than the superimposed WMF.[16] The Lorentz force, F_L, acting on the charged ions can increase the mass transport[28] and the magnetic field gradient force, F_B, tends to move paramagnetic Fe^{II} along the higher field gradient at the Fe^0 particle surface.[29] The uneven distribution of Fe^{II} will result in localized corrosion and thus corrosion is accelerated in the presence of WMF.[16] Moreover, pH at the Fe^0 particle surface in the presence of WMF should be lower than that in the absence of WMF, due to the increased mass transport of H^+ towards the Fe^0 particle surface caused by the additional convection induced by the F_L.[30] These speculations can reasonably explain the phenomena observed in our experiments, namely, a superimposed WMF could significantly improve the oxidative ability of Fe^0/H_2O_2 process toward 4-NP and widen the applicable pH range of Fe^0/H_2O_2 process.

3.3 Effect of the MF intensity on 4-NP Degradation in WMF-Fe^0/H_2O_2 Process.

Since the intensity of superimposed MF will influence the intensity of induced MF and the MF gradient around the iron spheres, the influence of the MF intensity on 4-NP degradation by WMF-Fe^0/H_2O_2 was investigated in a uniform MF and the results are presented in Figure 3. The inset in Fig. 3 shows the change of pseudo first-order degradation rate constants of 4-NP with MF intensity. The observed rate constants of 4-NP removal increased progressively from 0.0127 to 0.1018 min^{-1} by increasing the MF intensity from 0 to 20 mT, which may be ascribed to the larger F_L and F_B at higher MF intensity. To verify this point, the MF strength distributions of

the plane parallel to the applied homogeneous MF and through the center of a Fe^0 sphere and the MF gradients around a Fe^0 sphere when the flux densities of applied MF are 5 mT, 10 mT and 20 mT, respectively, were calculated by numerical simulations and presented in Fig. S6. Obviously, as the intensity of the applied uniform MF increased from 5 mT to 20 mT, the maximum MF intensity and gradient increased proportionally with increasing the intensity of applied MF and they appeared close to the Fe^0 particle surface. Consequently, the F_L acting on charged species and the F_B acting on paramagnetic ions would increase accordingly with increasing the intensity of applied MF and thus strengthen their influence on mass transport and the uneven distribution of paramagnetic ions (Fe^{II}) around Fe^0 particles.[16] Consequently, the accelerating effect of MF on 4-NP degradation by Fe^0-Fenton was increased with the intensity of MF. Nevertheless, a further increase in MF intensity from 20 mT to 40 mT had negligible influence on the rate constants of 4-NP degradation by Fe^0/H_2O_2. In addition, the rate constant of 4-NP oxidation by Fe^0/H_2O_2 was remarkably dropped from 0.1039 to 0.051 min^{-1} as the intensity of MF was elevated from 40 mT to 50 mT, which should be associated with the aggregation of Fe^0 particles in the uniform MF with intensity greater than 20 mT (as shown in Fig. S7). Therefore, the optimum intensity of MF for 4-NP degradation in WMF-Fe^0/H_2O_2 process was determined to be 20 mT in this study.

Figure 3.

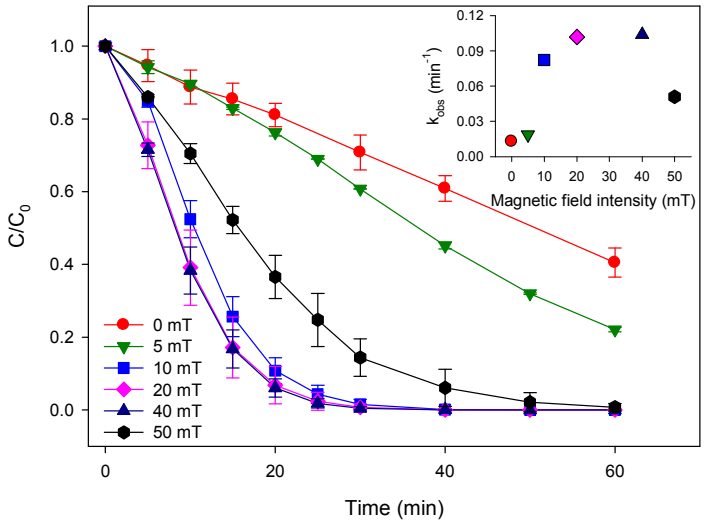

3.4 BBD and data analysis

Since it is very difficult to offer an uniform MF in practical application, the nonuniform WMF was employed in the Box-Behnken experimental design. Table 1 shows the design matrix applied and the actual experimental results (Y_{exp}) and data obtained from the BBD (Y_{calc}) for the response (Y) corresponding to the square root of k_{obs} of 4-NP degradation in WMF-Fe^0/H_2O_2 system. The coefficients of the response function (Eq. (7)) were obtained using experimental data and presented in Eq. (9).

$$Y = 0.7650 - 0.3127A + 0.8128B + 0.5322C - 0.1281AB - 0.1107AC - 0.0002BC + 0.0344A^2 - 0.0742B^2 + 0.0343C^2 \quad (9)$$

This model explains perfectly the results in the experimental range studied (R^2 adjusted = 0.93). Moreover, the model adequacy and significance was further evaluated by ANOVA, as shown in Table S3. The F-value of 24.62 and its p-value of 0.0002 (less than 0.05) implied the high significance of this model. Furthermore, the plot of experimental rate constants versus the predicted ones (Fig. S8) shows

satisfactory correlation (R^2 = 0.96). Therefore, this is a suitable model for predicting the removal rate constant under the investigated reaction conditions.

Table 1. Experimental data points used in the Box–Behnken design.

Run	Variable levels			k_{obs} (min^{-1})	R^2	Y_{exp}	Y_{pred}
	pH	Fe^0 (mM)	H_2O_2 (mM)				
1	2.0	0.10	0.55	0.2108	0.96	0.4591	0.5085
2	4.0	1.00	1.00	0.1055	0.97	0.3248	0.4058
3	2.0	1.00	0.55	0.9630	0.97	0.9813	0.9361
4	4.0	0.55	0.55	0.0806	0.94	0.2839	0.2621
5	6.0	1.00	0.55	0.0083	0.93	0.0911	0.0302
6	2.0	0.55	1.00	0.9155	0.99	0.9568	0.8972
7	2.0	0.55	0.10	0.3094	0.98	0.5562	0.5914
8	4.0	1.00	0.10	0.0881	0.95	0.2968	0.2992
9	6.0	0.55	1.00	0.0048	0.95	0.0693	0.0226
10	4.0	0.10	1.00	0.0494	0.95	0.2223	0.2087
11	4.0	0.55	0.55	0.0992	0.96	0.3150	0.2621
12	6.0	0.55	0.10	0.0045	0.96	0.0671	0.1153
13	6.0	0.10	0.55	0.0009	0.92	0.0300	0.0638
14	4.0	0.55	0.55	0.0650	0.93	0.2550	0.2621
15	4.0	0.10	0.10	0.0378	0.98	0.1944	0.1023
16	4.0	0.55	0.55	0.0544	0.93	0.2332	0.2621
17	4.0	0.55	0.55	0.0631	0.95	0.2512	0.2621

Note: $Y = Sqrt(k_{obs})$ ($\lambda = 0.5$)

The contour plots of the quadratic model with one variable kept at its central levels and the other two variables varying within the experimental ranges are shown in Fig. 4 and response surface plots are presented in Fig. S9. Obviously, the variation of the solution pH_{ini} remarkably affected the process efficiency, while the variations of Fe^0 and H_2O_2 dosages were less important. Lower pH_{ini} and larger dosages of Fe^0 and H_2O_2 were beneficial for 4-NP removal by WMF-Fe^0/H_2O_2 process within the range of variable chosen.

Figure 4.

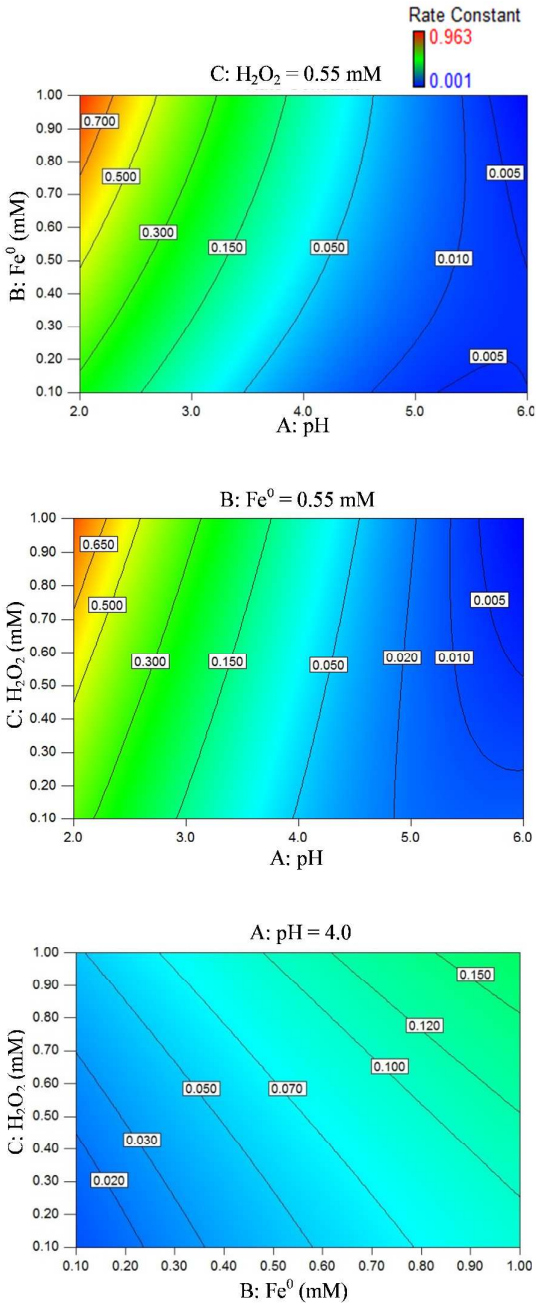

To test the reliability of the response functions predictions, three experiments different from BBD points were performed. It was found that the response function predictions (calculated by Eq. (9)) were in good agreement with the experimental results (as listed in Table S4), which confirmed the adequacy and validity of the model simulating the degradation rate of 4-NP in WMF-Fe^0/H_2O_2 system.

3.5 Possible degradation pathways of 4-NP

There have been some studies on identifying the degradation intermediates of 4-NP by advanced oxidation processes, which have been summarized in Table S5. Because different analytical methods, including GC-MS, LC-MS, and HPLC, had been employed in identifying the reaction intermediates and the mechanisms of 4-NP degradation in different AOPs were different, the amount and species of reaction intermediates detected in 4-NP degradation in different AOPs were very different.[31, 32] No one had studied the mechanisms of 4-NP degradation by Fe^0/H_2O_2 up to date and more importantly, the influence of WMF on degradation pathways of 4-NP by Fe^0/H_2O_2 needs clarification. Therefore, LC-MS/MS was employed to analyze the reaction intermediates of 4-NP in both Fe^0/H_2O_2 and WMF-Fe^0/H_2O_2 systems at pH_{ini} 4.0, based on which the 4-NP degradation pathways were proposed.

It was found that the application of WMF had no influence on the detected intermediate products, indicating that the application of WMF accelerated the removal of 4-NP while did not change the 4-NP degradation pathways. Six reaction intermediates were detected in the process of 4-NP oxidation besides the peak of 4-NP at m/z 139, as summarized in Table S5. Relying on the intermediates specified in this study and the reaction pathways of 4-NP in other AOPs,[32, 35, 38] the possible pathways of 4-NP degradation by Fe^0/H_2O_2 were proposed, as illustrated in Fig. 5. Two alternative pathways existed for the degradation of 4-CP in the Fe^0/H_2O_2 or WMF-Fe^0/H_2O_2 process.

Figure 5.

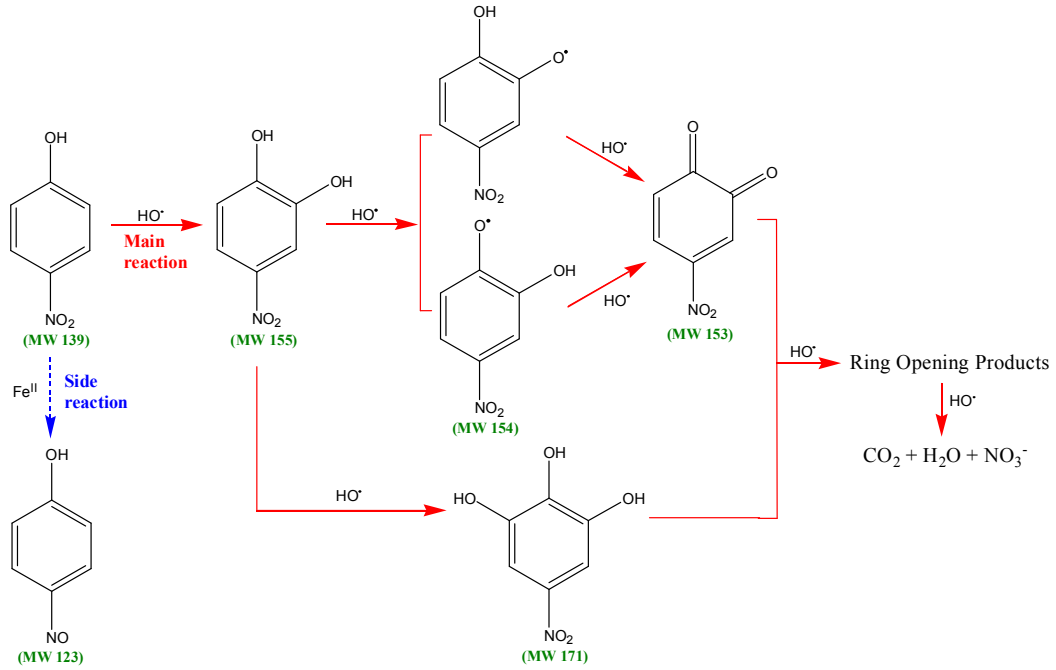

As described in the previous section, HO• was identified to be the major reactive species in both Fe^0/H_2O_2 and WMF-Fe^0/H_2O_2 processes at pH_{ini} 4.0 and thus the main reaction pathway was 4-CP oxidation by HO•. It is well known that the reaction of HO• with aromatic groups occurs via electrophilic addition.[31, 35, 39] HO• has a strong electrophilic character, and the attack of electrophilic HO• preferentially occurs at the ortho-position of the -OH group to form the corresponding OH-adduct, 4-nitrocatechol, as demonstrated in Fig. 5. On the subsequent HO• attack, the 4-nitrocatechol was converted into p-nitropyrogallol and o-nitrobenzoquinone, which were subjected to further attack by HO•, leading to the formation of nitro o-benzoquinone.[35] Alternatively, 4-nitrocatechol could be transformed to 4-nitropyrogallol by HO• oxidation.[40] The further oxidation of nitro o-benzoquinone and 4-nitropyrogallol by HO• resulted in the aromatic ring opening, formation of aliphatic acids, and eventual generation of mineralization products.[40, 41]

Besides the major oxidative degradation pathway, 4-NP could be degraded by

reduction since 4-nitrosophenol at low concentration was detected in the process of 4-NP removal by Fe^0/H_2O_2 or WMF-Fe^0/H_2O_2. This degradation intermediate was also observed in 4-NP removal by Fe^0 with ultrasonic irradiation and its appearance should be ascribed to the nascent Fe^{II} ions from the corrosion reaction of Fe^0.[38] But the nascent reductant was not enough to further reduce 4-nitrosophenol to 4-aminophenol in the Fe^0/H_2O_2 and WMF-Fe^0/H_2O_2 processes since 4-aminophenol was not detected. The minor removal of 4-NP (~4.5%) at pH_{ini} 4.0 in the presence of excessive TBA should be ascribed to the side reaction pathway.

3.6 Practical appliation prospect

In real practice, it's less likely to provide a magentic field around a treatment unit by applying electromagnetic field generator due to its high cost and energy use. Through our further studies, pretreatment of Fe^0 powder, which is ferromagnetic, in a magnetic field and then taking advantage of its residual magnetism may be a feasible method. As shown in Fig. S10, pre-magnetizing Fe^0 in a static and uniform magnetic field (MF) with the intensity of 100 or 300 mT remarkably improved the degradation rate of 4-NP by Fe^0/H_2O_2 process. Surprisingly, 4-NP was degraded by Fe^0/H_2O_2 process, which employed Fe^0 pre-magnetized in MF of 300 mT, at a similar rate as that by WMF-Fe^0/H_2O_2 process. Therefore, in real practice, the pre-magnetized Fe^0 may replace the pristine Fe^0 to enhance the performance of Fe^0/H_2O_2 process toward organic pollutants degradation, which is very easily applied. Further studies are still necessary to figure out the suitful and best working conditions to employ pre-magnetized Fe^0. In our lab, efforts are also being made on designing a continuous

flow reactor similar to the folded-plate flocculating tank with permanent magnets (low cost) to generate magnetic field, in case the Fe^0/H_2O_2 process with premagnetized Fe^0 could not decompose organic contaminant effectively.

4. Conclusions

The WMF induced a significant improvement in the oxidation rates of 4-NP by Fe^0/H_2O_2 and the enhancement was greater at higher pH_{ini}. $HO^{\bullet}$ was identified to be the primary oxidant responsible for the 4-NP degradation by either Fe^0/H_2O_2 or WMF-Fe^0/H_2O_2 at pH_{ini} 4.0 while both $HO^{\bullet}$ and Fe(IV) contributed to 4-NP degradation by WMF- Fe^0/H_2O_2 at pH_{ini} 6.0. The cumulative concentration of $HO^{\bullet}$ at pH_{ini} 4.0 in WMF-Fe^0/H_2O_2 system was about 3-fold of that in the Fe^0/H_2O_2 systems in 60 min, which may be associated with the accelerated Fe^0 corrosion and Fe^{II} generation, the limiting step of Fe^0/H_2O_2 process, in the presence of WMF. The application of WMF enhanced the mineralization of 4-NP by Fe^0/H_2O_2. Six reaction intermediates were detected in the process of 4-NP oxidation by Fe^0/H_2O_2 or WMF-Fe^0/H_2O_2 and the degradation pathways of 4-NP were proposed. The optimum intensity of MF for 4-NP oxidation by WMF-Fe^0/H_2O_2 was determined to be 20 mT and the MF with higher intensity would result in the aggregation of Fe^0 particles, which would deteriorate the 4-NP oxidation by WMF-Fe^0/H_2O_2. Lower pH and higher Fe^0 and H_2O_2 dosages were beneficial for 4-NP degradation by WMF-Fe^0/H_2O_2 and the derived RSM model could reasonably predict the rate constants of 4-NP oxidation in WMF-Fe^0/H_2O_2 system under the investigated reaction conditions. Hence, applying WMF to enhance the production of hydroxyl radical and broaden the working pH

range of Fe^0/H_2O_2 is efficient, energy-saving, chemical-free, and environmental friendly. The WMF-Fe^0/H_2O_2 technology will provide a new alternative to scientists working in the field of water treatment.

Acknowledgement

This work was supported the Specialized Research Fund for the Doctoral Program of Higher Education (20130072110026), the National Natural Science Foundation of China (21277095, 51478329), and Major Science and Technology Program for Water Pollution Control and Treatment (2012ZX07403-001).

References

1. M. Minella, G. Marchetti, E. De Laurentiis, M. Malandrino, V. Maurino, C. Minero, D. Vione and K. Hanna, *Appl. Catal. B-Environ.*, 2014, **154**, 102-109.
2. D. Guclu, N. Sirin, S. Sahinkaya and M. F. Sevimli, *Environ. Prog. Sustain.*, 2013, **32**, 176-180.
3. Y. L. Zhang, K. Zhang, C. M. Dai, X. F. Zhou and H. P. Si, *Chem. Eng. J.*, 2014, **244**, 438-445.
4. A. Goi and M. Trapido, *Chemosphere*, 2002, **46**, 913-922.
5. F. Lucking, H. Koser, M. Jank and A. Ritter, *Water Res.*, 1998, **32**, 2607-2614.
6. M. Kallel, C. Belaid, T. Mechichi, M. Ksibi and B. Elleuch, *Chem. Eng. J.*, 2009, **150**, 391-395.
7. L. J. Xu and J. L. Wang, *J. Hazard. Mater.*, 2011, **186**, 256-264.
8. H. Y. Li, Y. H. Gong, Q. Q. Huang and H. Zhang, *Ind. Eng. Chem. Res.*, 2013, **52**, 15560-15567.

9. J. G. Shi, Z. H. Ai and L. Z. Zhang, *Water Res.*, 2014, **59**, 145-153.

10. X. M. Xiong, B. Sun, J. Zhang, N. Y. Gao, J. M. Shen, J. L. Li and X. H. Guan, *Water Res.*, 2014, **62**, 53-62.

11. I. Grcic, S. Papic, K. Zizek and N. Koprivanac, *Chem. Eng. J.*, 2012, **195**, 77-90.

12. H. Zhang, J. H. Zhang, C. Y. Zhang, F. Liu and D. B. Zhang, *Ultrason. Sonochem.*, 2009, **16**, 325-330.

13. W. Wang, M. H. Zhou, Q. O. Mao, J. J. Yue and X. Wang, *Catal. Commun.*, 2010, **11**, 937-941.

14. Y. Tanimoto, A. Katsuki, H. Yano and S. Watanabe, *J. Phys. Chem. A*, 1997, **101**, 7359-7363.

15. L. P. Liang, W. Sun, X. H. Guan, Y. Y. Huang, W. Choi, H. L. Bao, L. N. Li and Z. Jiang, *Water Res.*, 2014, **49**, 371-380.

16. L. P. Liang, X. H. Guan, Z. Shi, J. L. Li, Y. N. Wu and P. G. Tratnyek, *Environ. Sci. Technol.*, 2014, **48**, 6326-6334.

17. Y. K. Sun, X. H. Guan, J. M. Wang, X. G. Meng, C. H. Xu and G. M. Zhou, *Environ. Sci. Technol.*, 2014, **48**, 6850-6858.

18. R. Hazime, Q. H. Nguyen, C. Ferronato, T. K. X. Huynh, F. Jaber and J. M. Chovelon, *Appl. Catal. B-Environ.*, 2013, **132**, 519-526.

19. I. Grčić, D. Vujević, J. Šepčić and N. Koprivanac, *J. Hazard. Mater.*, 2009, **170**, 954-961.

20. H. Liu, C. Wang, X. Z. Li, X. L. Xuan, C. C. Jiang and H. N. Cui, *Environ. Sci.*

Technol., 2007, **41**, 2937-2942.

21. J. Wu, H. Zhang, N. Oturan, Y. Wang, L. Chen and M. A. Oturan, *Chemosphere*, 2012, **87**, 614-620.

22. T. Zhou, Y. Z. Li, J. Ji, F. S. Wong and X. H. Lu, *Sep. Purif. Technol.*, 2008, **62**, 551-558.

23. J. J. Pignatello, D. Liu and P. Huston, *Environ. Sci. Technol.*, 1999, **33**, 1832-1839.

24. S. J. Hug and O. Leupin, *Environ. Sci. Technol.*, 2003, **37**, 2734-2742.

25. E. Finkelstein, G. M. Rosen and E. J. Rauckman, *J. Am. Chem. Soc.*, 1980, **102**, 4994-4999.

26. G. W. Klein, K. Bhatia, V. Madhavan and R. H. Schuler, *J. Phys. Chem.*, 1975, **79**, 1767-1774.

27. S. H. Joo, A. J. Feitz, D. L. Sedlak and T. D. Waite, *Environ. Sci. Technol.*, 2005, **39**, 1263-1268.

28. G. Hinds, J. Coey and M. Lyons, *Electrochem. Commun.*, 2001, **3**, 215-218.

29. M. Waskaas and Y. I. Kharkats, *J. Electroanal. Chem.*, 2001, **502**, 51-57.

30. J. A. Koza, M. Uhlemann, A. Gebert and L. Schultz, *J. Electroanal. Chem.*, 2008, **617**, 194-202.

31. M. A. Oturan, J. Peiroten, P. Chartrin and A. J. Acher, *Environ. Sci. Technol.*, 2000, **34**, 3474-3479.

32. W. Zhang, X. Xiao, T. An, Z. Song, J. Fu, G. Sheng and M. Cui, *J. Chem. Technol. Biotechnol.*, 2003, **78**, 788-794.

33. G. M. A. Kotronarou, and M. R. Hoffmann, *J. Phys. Chem.*, 1991, **95**, 3630-3638.

34. T. C. Wang, N. Lu, J. Li and Y. Wu, *Environ. Sci. Technol.*, 2011, **45**, 9301-9307.

35. V. Kavitha and K. Palanivelu, *J. Photochem. Photobiol., A*, 2005, **170**, 83-95.

36. Q. Z. Dai, L. C. Lei and X. W. Zhang, *Sep. Purif. Technol.*, 2008, **61**, 123-129.

37. H. X. Shi, X. W. Xu, X. H. Xu, D. H. Wang and Q. D. Wang, *J. Environ. Sci.-China*, 2005, **17**, 926-929.

38. B. Lai, Z. Y. Chen, Y. X. Zhou, P. Yang, J. L. Wang and Z. Q. Chen, *J. Hazard. Mater.*, 2013, **250-251**, 220-228.

39. Y. J. Liu, D. G. Wang, B. Sun and X. M. Zhu, *J. Hazard. Mater.*, 2010, **181**, 1010-1015.

40. W. B. Zhang, X. M. Xiao, T. C. An, Z. G. Song, J. M. Fu, G. Y. Sheng and M. C. Cui, *J. Chem. Technol. Biotechnol.*, 2003, **78**, 788-794.

41. N. Daneshvar, M. A. Behnajady and Y. Zorriyeh Asghar, *J. Hazard. Mater.*, 2007, **139**, 275-279.

Figure captions

Figure 1. (a) Influence of WMF on the pseudo first order rate constants of 4-NP degradation by Fe^0/H_2O_2 system at different pH_{ini} levels. Reaction conditions: $[4\text{-NP}]_0$ = 0.02 mM, $[H_2O_2]_0$ = 0.5 mM, $[Fe^0]_0$ = 0.5 mM, T = 25 ^oC; (b) Influence of WMF on mineralization of 4-NP by Fe^0/H_2O_2. Reaction conditions: $[4\text{-NP}]_0$ = 0.1 mM, $[H_2O_2]_0$ = 2.5 mM, $[Fe^0]_0$ = 2.5 mM, pH_{ini} = 4.0, T = 25 ^oC.

Figure 2. (a) Effect of radical quenching agent on 4-NP removal in Fe^0/H_2O_2 and WMF-Fe^0/H_2O_2 systems; (b) Comparison of the intensity of DMPO-OH adducts signals in Fe^0/H_2O_2 and WMF-Fe^0/H_2O_2 systems after 1 min. Reaction conditions: $[DMPO]_0$ = 100 mM, $[H_2O_2]_0$ = 30 mM, $[Fe^0]_0$ = 15 mM, pH_{ini} = 4.0; (c) Cumulative hydroxyl radical formation and p-HBA concentration over time; (d) Influence of WMF on dissolved ferric iron generation and H_2O_2 consumption in the Fe^0/H_2O_2 system. Reaction conditions for (a) (c) (d): $[TBA]_0$ = 0.1 M, $[BA]_0$ = 5 mM, $[4\text{-NP}]_0$ = 0.02 mM, $[H_2O_2]_0$ = 0.5 mM, $[Fe^0]_0$ = 0.5 mM, pH_{ini} = 4.0, T = 25 ^oC.

Figure 3. Influence of intensity of uniform MF on 4-NP degradation by WMF-Fe^0/H_2O_2 system. The inset shows the change of first-order degradation rate constants with MF intensity. Reaction conditions: $[4\text{-NP}]_0$ = 0.02 mM, $[H_2O_2]_0$ = 0.5 mM, $[Fe^0]_0$ = 0.5 mM, pH_{ini} = 4.0.

Figure 4. Contour plots of the rate constant of 4-NP for the three most important pair of factors

Figure 5. Possible degradation pathways of 4-NP in Fe^0/H_2O_2 and WMF-Fe^0/H_2O_2 systems.